Available online at www.sciencedirect.com
SCIENCE DIRECT®
Journal of Non-Crystalline Solids 336 (2004) 159–164
JOURNAL OF NON-CRYSTALLINE SOLIDS
www.elsevier.com/locate/jnoncrysol

Dielectric properties and structural features of barium-iron phosphate glasses

P. Bergo [a], S.T. Reis [b,*], W.M. Pontuschka [a], J.M. Prison [c], C.C. Motta [d]

[a] Institute of Physics, University of Sao Paulo, C.P. 66318, 05315-970 Sao Paulo, SP, Brazil
[b] Graduate Center for Materials Research, University of Missouri-Rolla, 301 Straumanis Hall, Rolla, MO 65409-1170, USA
[c] Energy and Nuclear Research Institute, C.P. 11049 Pinheiros, 05422-970 Sao Paulo, SP, Brazil
[d] Brazilian Navy Technological Center, C.P. 11049, 05598-900 Sao Paulo, SP, Brazil

Received 2 May 2003; received in revised form 9 February 2004

Abstract

The dielectric constant of barium-iron phosphate glasses with the general composition $(40-x)BaO \cdot xFe_2O_3 \cdot (60-x)P_2O_5$ has been investigated at two fixed frequencies (100 kHz and 9.0 GHz). The dielectric constant measured using microwave technique, and the ratio O/P of these glasses increase with increasing Fe_2O_3 content. The structure and valence states of the iron ions in these glasses were investigated using Mössbauer spectroscopy, infrared spectroscopy and differential thermal analysis. Both Fe(II) and Fe(III) ions present in these glasses in octahedral coordination act as permanent dipoles, and the increase of the iron concentration increase these permanent dipoles, contributing to the dielectric constant.

1. Introduction

Many phosphate glasses have a chemical durability usually inferior to that of most silicate and borosilicate glasses, but iron phosphate glasses are an exception [1]. In addition to their generally excellent chemical durability, iron phosphate glasses have low melting temperature, typically between 950 and 1150 °C. Investigations of iron phosphate wasteforms obtained by adding different amounts of various simulated nuclear wastes to a base iron phosphate glass, whose composition is $40Fe_2O_3 \cdot 60P_2O_5$ (mol%) showed that these glassy wasteforms have a corrosion rate up to one thousand times lower than that of a comparable borosilicate glass [2–4].

Family of phosphate glasses with an O/P ratio of 3.5 based on pyrophosphate (P_2O_7) groups is chemically more stable in aqueous solutions compared to phosphate glasses with an O/P ratio different of 3.5. Because of their unusually high chemical durability and other properties, iron-phosphate glasses [2] and lead-iron-phosphate glasses [5] are of interest for nuclear waste immobilization.

The most extensive use of phosphate glasses for vitrifying nuclear wastes has occurred in the former Soviet Union [6], where several hundred tons of nuclear waste has been immobilized in a sodium aluminophosphate glass. In recent years, it has been found that iron phosphate glasses of composition $40Fe_2O_3 \cdot 60P_2O_5$ (mol%) can accommodate in excess of 50% of certain HLW constituents while maintaining excellent chemical durability [7]. For another hand, the waste vitrification in iron phosphate glasses offers the advantage that the some kind of wastes provide considerable amount of the components (Fe_2O_3, P_2O_5) needed for glass formation, thereby decreasing the volume of the final waste product.

The microwave vitrification has many advantages over conventional joule-heated melters [8]. Conventional joule heating requires electrodes in direct contact with the glass limiting the service life of these melters. Microwave vitrification is electrodeless because microwave energy is absorbed directly by the glass with efficiently and faster temperature control compared to conventional radiant heating. For joule-heating, the entire melter must be brought to a working temperature

* Corresponding author. Tel.: +1-573 341 4359; fax: +1-573 341 2071.
E-mail address: reis@umr.edu (S.T. Reis).

0022-3093/$ - see front matter © 2004 Elsevier B.V. All rights reserved.
doi:10.1016/j.jnoncrysol.2004.02.008

over a period of several days to avoid cracking the melter refractory insulation but the microwave melters can be brought to temperatures in minutes because internal refractory insulation is not required [9]. In this case, the microwave properties including relative dielectric constant, quality factor and the temperature coefficient of frequency (TCF), become important factors determining the glass processing in microwave oven [10]. There are relatively few investigations of the microwave properties of phosphate glasses reported in literature [11,12]. However these investigations are mainly focused on high aluminoborosilicate glasses which had higher softening temperatures. Thus, knowledge of the microwaves effects in these glasses may indicate modifications of compositions and processing conditions, which could expand their applications.

The purpose of the present work was to investigate the dielectric properties of barium-iron phosphate glasses and to relate these properties to the structure of the glass using Mössbauer and IR spectroscopies, and DTA.

2. Experimental procedure

Barium-iron phosphate glasses with the composition $(40-x)BaO \cdot xFe_2O_3 \cdot (60-x)P_2O_5$, $0 \leqslant x \leqslant 15.5$ (mol%), were prepared by melting homogeneous mixtures of reagent grade $BaCO_3$, Fe_2O_3, and $NH_4H_2PO_4$ in dense alumina crucibles at 1000 °C in air for 2 h. The melt was quenched in air by pouring it into a steel mold to form bars of 1 cm × 1 cm × 5 cm. The bars were immediately transferred to a furnace and annealed at 450 °C for 2 h. Table 1 gives the batch composition and raw materials used.

All the DTA (Perkin–Elmer, Model DT7) experiments were conducted at a heating rate of 10 °C/min in flowing (20 cm^3/min) nitrogen gas using alumina crucibles. A high purity (99.999%) alumina powder was used as the reference material. The DTA machine was calibrated periodically for temperature using the melting points of In, Al, and Au. The estimated error in glass transition temperature (T_g) and crystallization temperature (T_c) is ±2 °C. Room temperature XRD patterns for glass samples were collected using an X-ray diffractometer (Scintag XDS2000).

The infrared (IR) spectrum for each glass was measured between 450 and 1500 cm^{-1} using a Perkin–Elmer 1760X FT-IR spectrometer. Samples were prepared as pellets by pressing a mixture of about 4 mg of glass powder and 150 mg of anhydrous KBr powder. The spectrometer was purged with dry nitrogen while 20 scans were collected for each glass. The spectrum for pure KBr was subtracted from each glass spectrum to correct the background.

The Mössbauer spectra were obtained at room temperature on a spectrometer (ASA 600) which utilized a room temperature 50 mCi cobalt-57 source embedded in a rhodium matrix. The spectrometer was calibrated at 23 °C with α-iron foil and the line width of the α-iron spectrum was 0.27 mm/s. Mössbauer absorbers of approximate thickness 140 mg/cm^2 were prepared using 200 mesh powders. The Mössbauer spectra were fit with broadened paramagnetic Lorentzian doublets. This fitting method has been proved to give reliable hyperfine parameters [13]. Details of this fitting procedure have been discussed previously [14].

The procedures for the microwave measurements were reported previously [15] and described here briefly.

Table 1
Batch composition and properties of iron-barium phosphate glasses

	V0	V1	V2	V3	V4	V5	V6
Glass (mol%)							
P_2O_5	60.0	58.08	56.16	54.60	53.40	51.90	50.70
Fe_2O_3	0	3.20	6.40	9.00	11.00	13.50	15.50
BaO	40.0	38.72	37.44	36.40	35.60	34.60	33.80
Batch (wt%)							
$NH_4H_2PO_4$	94.22	90.94	87.68	85.05	83.03	80.52	78.52
Fe_2O_3	–	3.48	6.94	9.73	11.87	14.54	16.66
$BaCO_3$	53.88	52.01	50.14	48.64	47.48	46.05	44.90
Properties							
O/P ratio[a]	2.83	2.92	3.00	3.08	3.14	3.22	3.29
(Fe)/P[a]	0	0.05	0.11	0.17	0.21	0.26	0.31
T_g (°C)	508	509	512	522	530	529	530
T_c (°C)	703	706	708	715	730	731	730
Fe(II)/(Fe(II)+Fe(III))[b]	–	1.4	4.1	5.3	6.2	8.7	10.3
ε (100 kHz)[c]	5.00	5.23	5.20	5.18	5.37	5.52	5.85
ε (9 GHz)[c]	1.91	2.02	2.06	1.99	1.99	2.11	2.18

[a] Molar ratio of oxygen to phosphorus (O/P) and (Fe)/P molar ratio were calculated from the batch compositions.
[b] Fe(II) ratio calculated from the Mössbauer results.
[c] Dielectric constant in arbitrary units.

In order to measure the dielectric constant in the microwave region, the technique of shorted-circuit was used. In this technique, the sample is placed against the short-circuit inside a wave guide. The standing wave is measured using a slotted wave guide in with a detector and a microwave probe is used to measure the microwave signal. The signal obtained from the detector can be measured by ordinary methods. The standing wave is measured in absence and presence of the sample. The minima in the standing wave will shift by an amount Δl, and this amount is proportional to the dielectric constant of the sample. Fig. 1 shows the microwave setup used for the measurements.

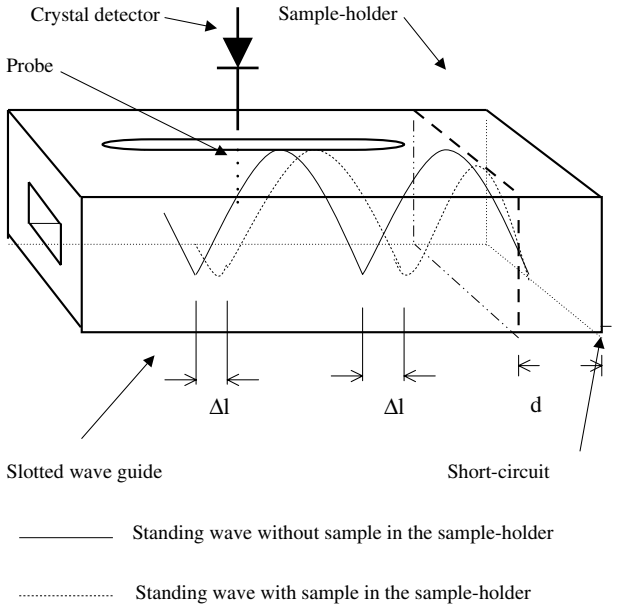

Fig. 1. Microwave setup for the measurements.

3. Results

3.1. DTA and X-ray diffraction

All of the compositions listed in Table 1 formed glass as no crystalline phase was detected by X-ray diffraction. It is well-known that the changes in phosphate structure are strongly influenced by the overall O/P ratio [16]. It was, also, found that the glass-forming tendency decreases with the increasing O/P ratio [17].

Fig. 2 shows the DTA patterns for the base glass, V0, and glasses with increasing Fe_2O_3 content from 6.4 to 15.5, V2 to V6, respectively. Samples V1, V3, and V5 are not shown. As shown by small endothermic peaks, the glass transition temperature, T_g, for the V0 to V6 glasses increases between 508 and 530 °C. For the ultraphosphate [18] glasses with $O/P < 3$ (V0 and V1) the exothermic peaks at 703 and 708, respectively, are due to the crystallization of Q^3 tetrahedra. The metaphosphate $O/P = 3$ (V2) and polyphosphate glasses [18] $O/P > 3$ (V3, V4, V5 and V6) the exothermic peaks between 708

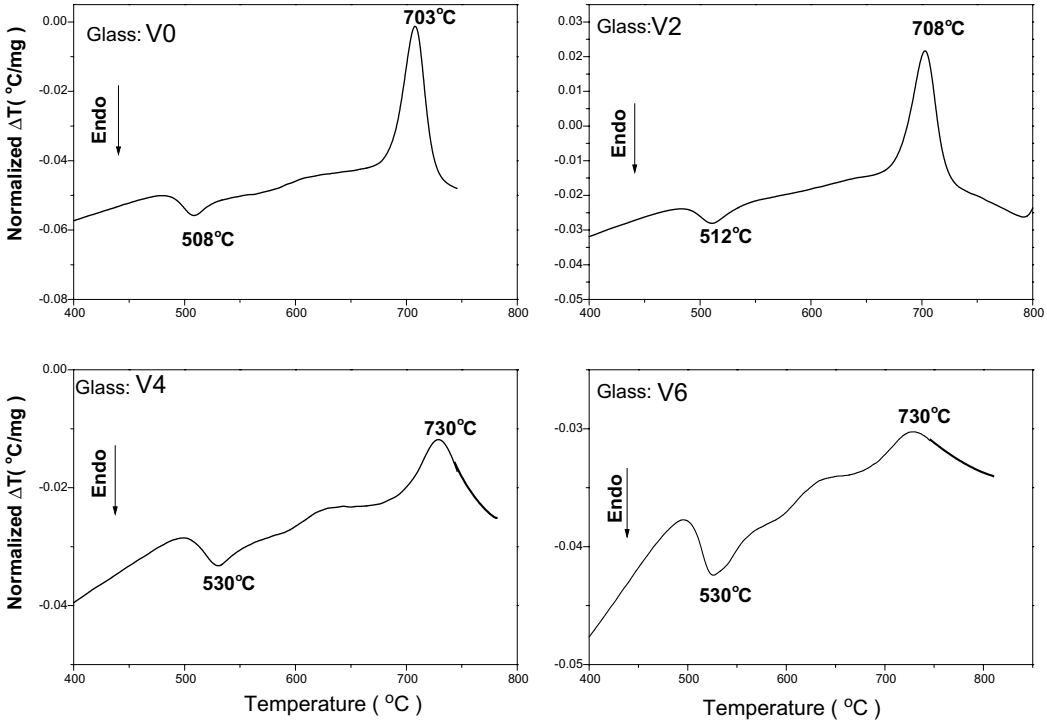

Fig. 2. Differential thermal analysis (DTA) curve for iron-barium phosphate glasses.

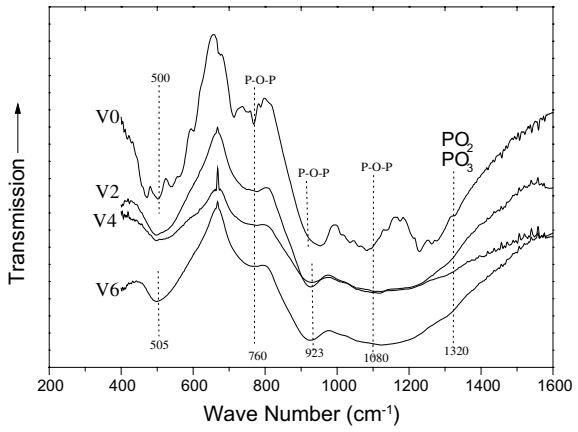

Fig. 3. The IR spectra of barium-iron phosphate glasses.

and 730 °C, are due to the crystallization of Q^2 and Q^1 structures respectively. These results are confirmed by IR spectroscopy (see Fig. 3).

3.2. IR and Mössbauer measurements

The IR spectra of all four glasses are shown in Fig. 3. The spectra are very similar to those reported for other phosphate glasses [19–21]. The band around 500 cm^{-1} may be due to overlapping vibrations of iron oxygen polyhedra and pyrophosphate (Q^1) groups [21,22]. The band at 760 cm^{-1} is assigned to the symmetric stretching vibration of the P–O–P bridge [21], while the band at 923 cm^{-1} is assigned to the asymmetric stretching vibration of P–O–P bridge [21,22]. The bands observed at ~1080 and 1330 cm^{-1} are attributed to the symmetric and asymmetric vibrations of Q^3 and Q^2 groups, respectively [22].

The room temperature Mössbauer spectra of the V1, V2, V4 and V6 barium-iron phosphate glasses samples are shown in Fig. 4, samples V3 and V5 are not shown. The iron valence and hyperfine parameters, isomer shift δ and quadruple splitting ΔE_Q, calculated from the Mössbauer spectra are given in Table 2. Some of the Fe(III) ions in the starting batch are reduced to Fe(II) ions during melting as the Mössbauer spectra indicate that all the glasses contain from 1.4% to 10.3% of Fe(II). The isomer shift for Fe(II) and Fe(III) ranges from 0.95 to 1.19 and from 0.39 to 0.42 mm/s, respectively, while the quadruple splitting ranges from 1.99 to 2.36 mm/s and from 0.81 to 0.94, respectively. These values for the isomer shift correspond to octahedral coordination for both Fe(II) and Fe(III) ions in these glasses.

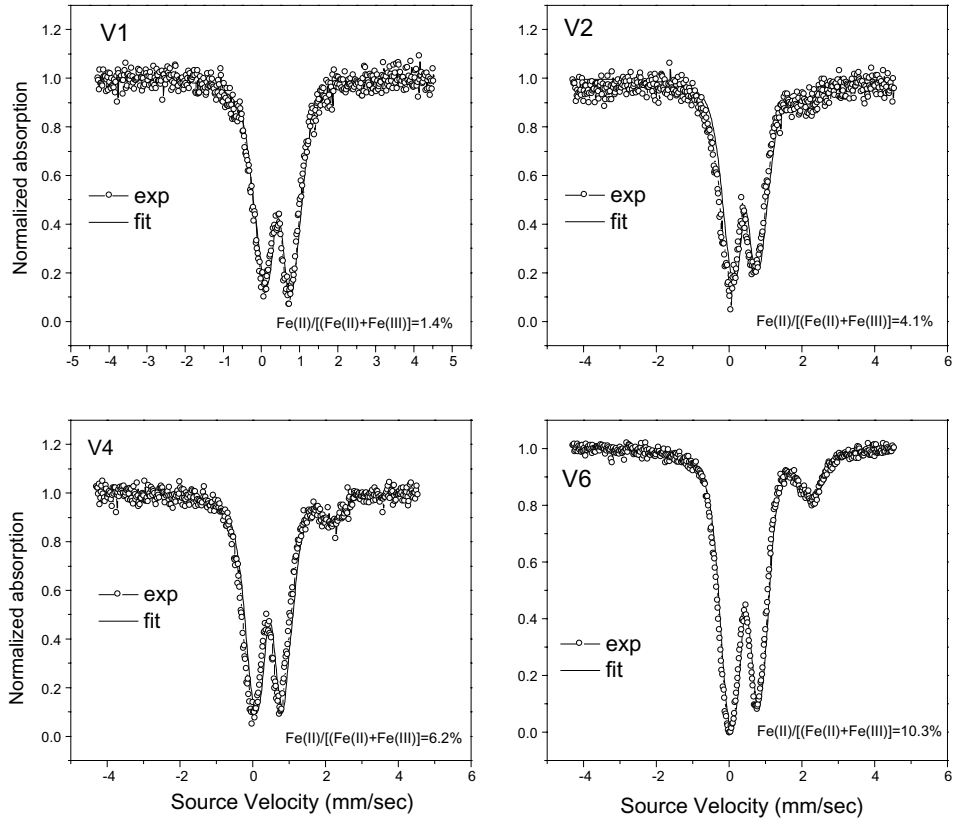

Fig. 4. Mössbauer spectra measured at 23 °C for $(40-x)BaO \cdot xFe_2O_3 \cdot (60-x)P_2O_5$ glasses.

Table 2
Room temperature Mössbauer hyperfine parameters, isomer shifts $\langle\delta\rangle$, quadruple splitting $\langle\Delta E_Q\rangle$, fraction of Fe(II) and melting temperatures for barium-iron phosphate glasses

Glass	$\langle\delta\rangle$ (mm/s)		$\langle\Delta E_Q\rangle$ (mm/s)		Fraction[a] of Fe(II) (%)
	Fe(II)	Fe(III)	Fe(II)	Fe(III)	Fe(II)
V1	1.18	0.40	2.08	0.94	1.4
V2	0.95	0.41	2.16	0.89	4.1
V3	0.95	0.42	2.15	0.89	5.3
V4	0.95	0.42	2.36	0.81	6.2
V5	0.94	0.41	2.36	0.82	8.7
V6	1.19	0.39	1.99	0.93	10.3

The estimated error in $\langle\delta\rangle$ and $\langle\Delta E_Q\rangle$ is ±0.03 mm/s.
[a] Calculated from the Mössbauer spectra.

3.3. Dielectric constants

Fig. 5 shows the relative dielectric constants at 100 kHz and 9 GHz of barium-iron phosphate as a function of Fe_2O_3 content, indicating that the variation in Fe_2O_3 content causes only a slight change of relative dielectric constant. The values for dielectric constants also are given in Table 1. The change is not constant for different concentrations of Fe_2O_3 at frequency of 100 kHz, indicating that at low frequencies the atoms and molecules could be polarized easily and in the microwave region only electronic polarization occurs [23]. This is due to the structural relaxation time being connected to the dipolar polarization. The time required to small induced dipoles to attain the equilibrium position as a response to variations of an external electric field is of order of 10^{-10} to 10^{-15} s, whereas the time required to large molecules is of the order of second, hours and more. For this reason, at higher frequencies, the dielectric constant decreases, as seen in these results. The error bars in the Fig. 4 for the experimental data are smaller than the size of the symbols.

The O/P ratio dependence of the dielectric constant, ε, measured at 100 kHz for all glasses is shown in Fig. 6. At O/P < 3.0, ε approaches its constant value which is probably result of lower concentration of Fe(II) or Fe(III) in these glasses. The barium-iron phosphate with O/P < 3.0, like other ultraphosphate glasses [18] have networks that are cross-linked by Q^3 tetrahedra which form chains, rings or isolated PO_4 groups. With addition of iron content, the P–O–P bonds are replaced by P–O–Fe(II) and/or P–O–Fe(III) bonds, increasing the O/P ratio and the ε due to electrode polarization of the phosphate anions interconnected through terminal oxygens by ionic bonds with Fe(II) and/or Fe(III) cations.

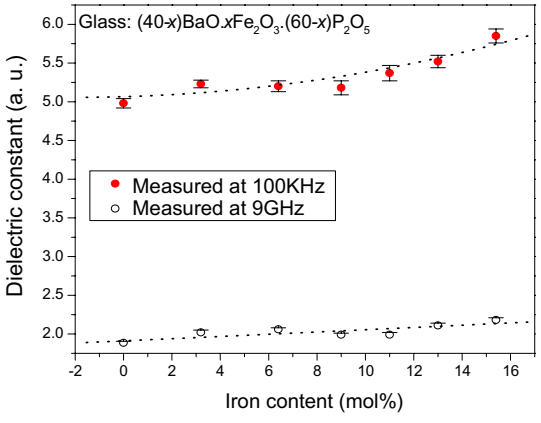

Fig. 5. Dielectric constant (ε) of iron-barium phosphate glasses in function of iron content.

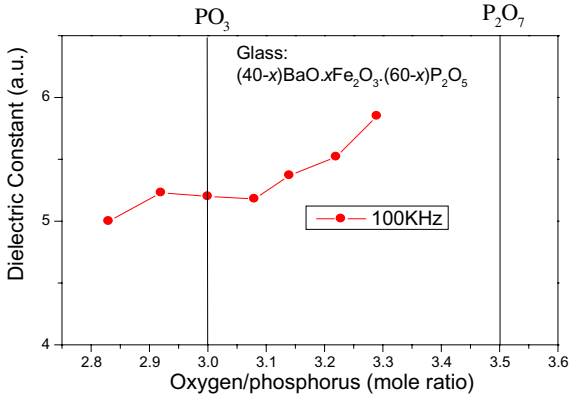

Fig. 6. Dependence of dielectric constant (ε) of iron-barium phosphate glasses on the oxygen to phosphorus molar ratio.

4. Discussion

The increase in the dielectric constant of barium-iron phosphate glasses is attributed to the replacement of P–O–P bonds by more susceptive Fe–O–P bonds to the microwave effect. As the Fe_2O_3 content in the glass increases, the number of Fe–O–P bonds also increases. It was found that the V6 glass, where the O/P is 3.3 has the highest dielectric constant at 100 kHz.

Glasses with an O/P ratio less than 3.0 (V0 and V1) have structures approaching the ultraphosphate composition which consists of long chains of PO_4 groups

and contains more P–O–P bonds. These glasses have a lower dielectric constant compared to the glass with O/P ratio >3.0 whose structure is closer to the pyrophosphate composition (P_2O_7) [15]. In fact, the V6 glass (O/P = 3.3) had the highest dielectric constant with ε of 2.18 (9 GHz) and 5.85 (100 kHz).

The IR spectra show that the band around 505 cm^{-1} (V2, V4 and V6 glassy samples) is due to overlapping vibrations of iron oxygen polyhedra and P_2O_7 groups. In general this band is related to the number of Fe–O–P bonds present in glasses with high Fe_2O_3 content [1,2,5]. However there are no significant differences in the spectra between these glassy samples containing different amount of iron (6.0%, 11.0% and 15.5% respectively).

The IR band at 760 cm^{-1}, which is due to symmetric stretching of P–O–P bonds [24,25] is a result of the larger number of Fe–O–P bonds, which replace the bridging P–O–P bonds in these glasses with increasing (Fe)/P ratio (Fe/P ratio is 0.11 and 0.31 for the V2 and V6 glasses, respectively).

The general structure of the barium-iron phosphate glasses can be visualized as consisting of PO_4 tetrahedra joined together by oxygen polyhedra which contain Fe(II) and Fe(III) and Ba^{2+} ions in interstitial positions which act as a modifier in the glass network.

The Mössbauer results indicate that even though there is no Fe(II) in the starting batch, the as-annealed glasses contain from 1.4% to 10.3% Fe(II) due to a reduction of a portion of the Fe(III) ions during melting in air. The isomer shift $\langle\delta\rangle$ values in Table 2 indicate that both Fe(II) and Fe(III) ions have oxygen neighbors in octahedral coordination. The quadruple splitting measured for the glasses in the present study are in the range of 1.99–2.36 mm/s which indicates that the Fe(II) environment in the glass is different from that in crystalline $Fe_3(P_2O_7)_2$ [5], i.e., the Fe(II) ions are unlikely to be in well-defined trigonal prism coordination in the glass.

5. Conclusions

The structure and dielectric properties of barium-iron-phosphate glasses have been investigated using various techniques. The increasing in the dielectric constant with the iron content is attributed to the P–O–P bonds being replaced by Fe(II and/or III)–O–P bonds. The barium-iron phosphate glasses consist of PO_4 tetrahedra joined together by oxygen polyhedra which contain Fe(II) and Fe(III) and Ba^{2+} ions in interstitial positions which act as a modifier in the glass network. The ions iron (II and/or III) in octahedral coordination act as permanent dipoles, and the increase of the iron concentration increase these permanent dipoles, contributing to the dielectric constant. Another interesting result is the increasing of the amount of Fe(II) and the increasing observed on the dielectric properties, however the reason for this in not clear at this time.

Acknowledgements

One of the authors P. Bergo thanks Fundacão de Amparo a Pesquisa do Estado de São Paulo (FAPESP) for a doctoral fellowship as well as the support from the Institute of Physics – University of Sao Paulo – Brazil which has made this work possible.

References

[1] G.K. Marasinghe, M. Karabulut, C.S. Ray, D.E. Day, J. Non-Cryst. Solids 263&264 (2000) 146.
[2] M. Karabulut, G.K. Marasinghe, P.G. Allen, C.H. Booth, M. Grimsditch, J. Mater. Res. 15 (2000) 1972.
[3] M.G. Mesko, D.E. Day, J. Non-Cryst. Solids 273 (1999) 27.
[4] D.E. Day, Z. Wu, C.S. Ray, P. Hrma, J. Non-Cryst. Solids 241 (1998) 1.
[5] S.T. Reis, M. Karabulut, D.E. Day, J. Nucl. Mater. 304 (2002) 87.
[6] A.S. Polyakov, G.B. Borisov, N.I. Moiseenko, V.I. Osnovin, E.G. Dzenkun, At. Energ. 76 (3) (1994) 183.
[7] D.E. Day, Z. Wu, C.S. Ray, P. Hirma, J. Non-Cryst. Solids 241 (1997) 1.
[8] R.G. Baxter, Design and Construction of the Defense Waste Processing Facility Project at the Savannah River Plant, in: Proc. 15th Symp. on Waste Management, Tucson, AZ, Am. Nucl. Soc., February 26–March 2, 1989.
[9] T.L. White, W.D. Bostick, C.T. Wilson, C.R. Schaich, Design of Microwave Vitrification Systems for Radioactive Waste, Oak Ridge National Laboratory, Oak Ridge, TN 37831-8071, CONF-9511189-1.
[10] J.M. Wu, M.C. Chang, P. Yao, J. Am. Ceram. Soc. 73 (1990) 1599.
[11] A.R. von Hippel, in: A.R. Von Hippel (Ed.), Dielectric Materials and Applications, Technology Press of MIT and Wiley, Cambridge, MA and New York, 1954.
[12] L. Navias, R.L. Grenn, J. Am. Ceram. Soc. 29 (1946) 267.
[13] C.S. Ray, X. Fang, M. Karabulut, G.K. Marasinghe, D.E. Day, J. Non-Cryst. Solids 249 (1999) 1.
[14] G.K. Marasinghe, M. Karabulut, C.S. Ray, D.E. Day, C.H. Booth, P.G. Allen, D.K. Shuh, Ceram. Trans. 87 (1998) 261.
[15] S. Roberts, A. Von Hippel, J. Appl. Phys. 17 (1946) 610.
[16] A. Moguš-Milanković, B. Pivac, K. Furić, D.E. Day, Phys. Chem. Glasses 38 (1997) 74.
[17] S.T. Reis, M. Karabulut, D.E. Day, J. Nucl. Mater. 304 (2002) 87.
[18] J. Hudgens, R.K. Brow, D.R. Tallant, S.W. Martin, J. Non-Cryst. Solids 223 (1998) 21.
[19] X. Fang, C.S. Ray, G.K. Marasinghe, D.E. Day, J. Non-Cryst. Solids 263&264 (2000) 293.
[20] G.J. Exarhos, P.J. Miller, W.M. Risen Jr., J. Chem. Phys. 60 (1974) 4145.
[21] J.J. Hudgens, S.W. Martin, J. Am. Ceram. Soc. 76 (1993) 1691.
[22] M. Karabulut, G.K. Marasinghe, P.G. Allen, C.H. Booth, M. Grimsditch, J Mater. Res. 15 (2000) 1972.
[23] Fröhlich, Theory of Dielectrics, McGraw Hill, 1958.
[24] G. Wang, Y. Wang, B. Jin, SPIE 2287 (1994) 214.
[25] J. Hudgens, R.K. Brow, D.R. Tallant, S.W. Martin, J. Non-Cryst. Solids 223 (1998) 21.